Supplemental Information for Viscosity Reduction in HPAM Solutions Induced by Silica Nanoparticle Additives

Mingbao Zhang, Xukang Lu, Moran Wang†
Department of Engineering Mechanics, Tsinghua University, Beijing 100084, China

I. Supplementary Frequency-Sweep Measurements of G' and G''

Dynamic oscillatory rheology was performed to further characterize the viscoelastic response of HPAM solutions across polymer concentrations. Frequency-sweep measurements were carried out to obtain the storage and loss moduli, G' and G'', over the accessible frequency window. As shown in Fig. S1a and Fig. S1b, clear $G' - G''$ crossovers are observed for the 500 ppm and 1000 ppm solutions, respectively, indicating the emergence of an elastic contribution with increasing frequency. Notably, the crossover shifts to higher frequencies at 500 ppm and moves toward lower frequencies at 1000 ppm, suggesting a pronounced increase in the characteristic relaxation time as the polymer concentration increases. For the 5000 ppm solution (Fig. S1c), G' remains higher than G'' throughout the entire measurable frequency range, implying that the terminal regime is shifted below the instrument's low-frequency limit and that the viscoelastic response is dominated by elastic storage within the experimental window.

To quantify the concentration-dependent transition, the crossover frequency $f_{cross}$was extracted when applicable, and the corresponding relaxation time was estimated as $\tau = \frac{1}{f_{cross}}$. The resulting $\tau(c_p)$ trend is summarized in Fig. S1d, where a pronounced increase in relaxation time is observed around 1000 ppm, consistent with an apparent crossover toward entanglement-dominated viscoelasticity for the present HPAM system[1] under the investigated conditions.

† Corresponding author; Email: mrwang@tsinghua.edu.cn

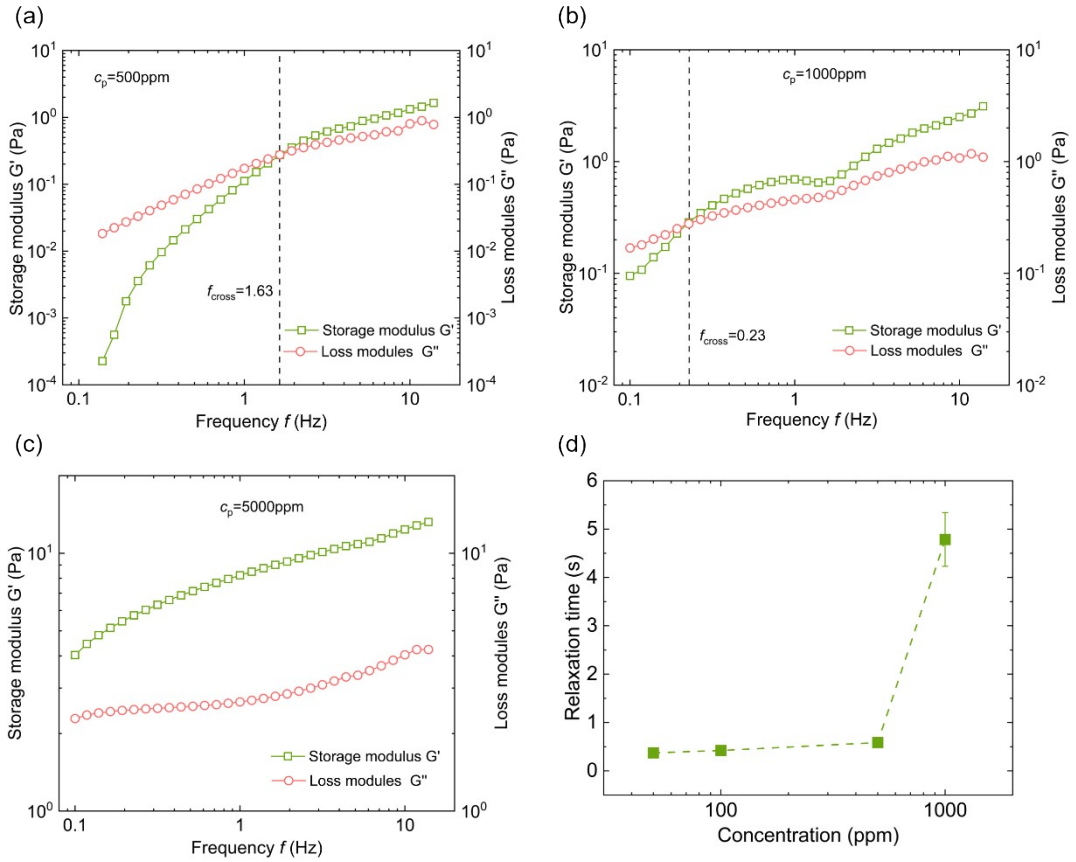

Fig. S1. Frequency-sweep measurements of the storage and loss moduli, G' and G'', for HPAM solutions at (a) 500 ppm, (b) 1000 ppm, and (c) 5000 ppm. (d) Relaxation time τ as a function of polymer concentration.

II. Additional Rheological Data with Different Silica Nanoparticle Sizes

The Supplementary rheological measurements were performed for silica nanoparticles with different particle sizes (5 nm, 50 nm, and 180 nm), and the resulting zero-shear viscosity η_0 is summarized in Fig. S2. The orange line and shaded band represent the mean η_0 of the nanoparticle-free HPAM solution (PS) and the associated experimental uncertainty (mean ± error), respectively. For all tested particle sizes, η_0 decreases with increasing nanoparticle concentration c_n, and the measured values fall below the PS baseline at sufficiently high c_n. These results indicate that the viscosity-reduction trend is reproducible and remains robust within the investigated HPAM–silica system.

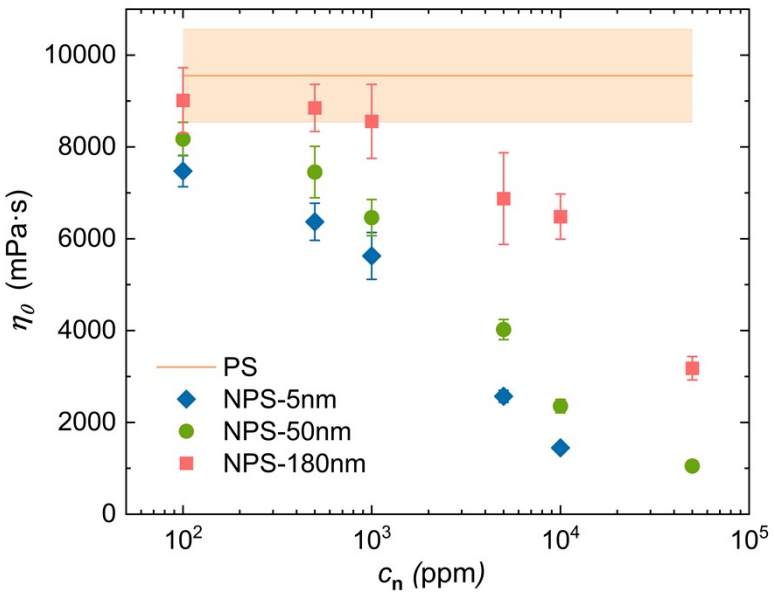

Fig. S2. Dependence of zero-shear viscosity η_0 on nanoparticle concentration c_n for HPAM solutions containing silica nanoparticles of different particle sizes (5, 50, and 180 nm). Error bars indicate measurement variability, and the orange line/shaded band shows the nanoparticle-free HPAM baseline (PS; mean ± error).

III. Effect of Ionic Conductivity and pH on the Rheology of HPAM Solutions

To evaluate whether the viscosity reduction observed upon the addition of silica nanoparticles can be fully attributed to changes in ionic conditions, the ionic conductivity and pH of HPAM solutions containing different concentrations of silica nanoparticles were systematically examined. As shown in Fig. S3a, the ionic conductivity increases monotonically with increasing nanoparticle concentration, indicating an increase in the concentration of mobile ions in the system.

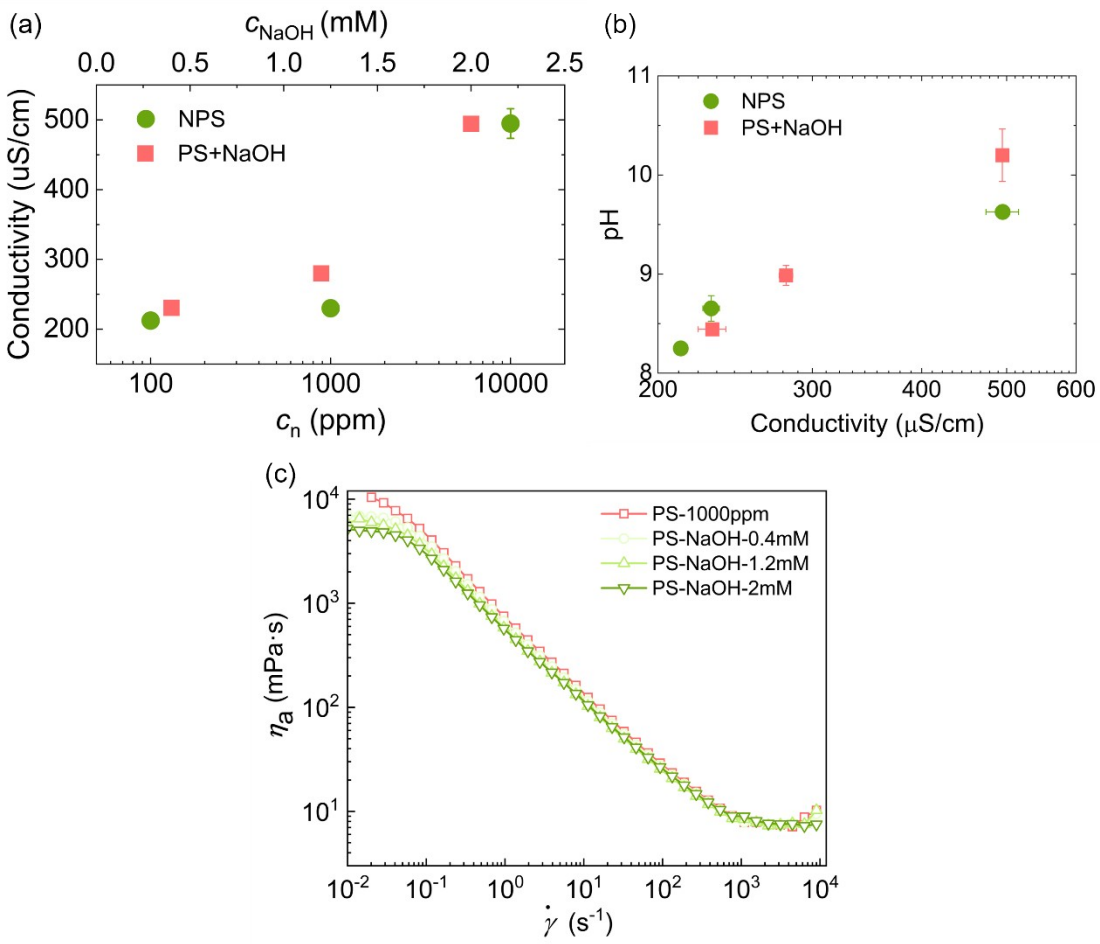

Fig. S3. (a) Ionic conductivity of HPAM solutions as a function of silica nanoparticle concentration. (b) pH and ionic conductivity of nanoparticle-free HPAM solutions adjusted by NaOH to match the values measured in silica-containing samples. (c) Apparent viscosity of the conductivity- and pH-matched control solutions compared with HPAM solutions measured under identical rheological conditions.

The origin of this conductivity increase can be traced to the stabilization mechanism of colloidal silica dispersions. The silica nanoparticles used in this work are stabilized under mildly alkaline conditions, a common practice achieved by adjusting the dispersion using bases such as NaOH or ammonia/amine species. Under these conditions, surface silanol groups undergo deprotonation ($\equiv Si-OH \rightarrow \equiv Si-O^-$), leading to enhanced surface charge and electrostatic stabilization. This process is accompanied by counterions and may introduce a small amount of residual electrolyte (primarily Na^+), which contributes to the measured ionic conductivity. Consistent with this interpretation, a slight increase in solution pH is also observed after nanoparticle addition.

To evaluate whether the observed changes in pH and ionic conductivity alone are sufficient to explain the viscosity reduction, a matched-control experiment was performed. Specifically, NaOH was added to nanoparticle-free HPAM solutions to adjust both the pH and ionic conductivity to match those measured in the corresponding silica-containing samples. The resulting pH and conductivity values are summarized in Fig. S3b. Rheological measurements were then conducted on these conductivity- and pH-matched control solutions under identical conditions, with the apparent viscosity results shown in Fig. S3c.

The control experiments demonstrate that ion- and pH-related effects can indeed induce a measurable decrease in viscosity, indicating that ionic conditions contribute to the baseline rheological response of HPAM solutions. However, even under matched pH and conductivity conditions, the magnitude of viscosity reduction remains substantially smaller than that observed in the presence of silica nanoparticles. This comparison indicates that the conductivity increase associated with nanoparticle addition is not sufficient to account for the full extent of the viscosity reduction, supporting the presence of an additional nanoparticle-mediated contribution beyond simple ionic screening effects.

IV. FT-IR Spectral Comparison of HPAM and HPAM–SiO_2 Mixtures and Evidence for Enhanced Hydrogen Bonding

Fig. S4 compares the FT-IR spectra of the pure HPAM solution and the HPAM–SiO_2 mixture. Fig. S4(a) shows the raw spectra, highlighting the overall absorption features as well as baseline differences arising from the solution background, bound water and nanoparticle-related scattering. Fig. S4(b) presents a magnified view of the 1550-1750 cm^{-1} region (amide bands), which mainly contains the HPAM Amide I band ($C=O$ stretching, ~1650 cm^{-1}) and Amide II band ($N-H$ bending/$C-N$ stretching, ~1550 cm^{-1}). To enable a robust comparison of peak positions and shapes, a local linear baseline correction was applied within the selected window by subtracting the straight

line connecting the two endpoints, followed by optional peak-height normalization within the Amide I window. A pronounced red shift of the Amide I band (~16 cm^{-1}) is observed upon adding SiO_2, indicating a strengthened hydrogen-bonding environment around the carbonyl groups ($C=O$ acting as a hydrogen-bond acceptor interacting with silanol groups and/or bound water on silica surfaces). Fig. S4(c) shows the magnified 3000-3700 cm^{-1} region corresponding to $O-H/N-H$ stretching vibrations, processed using the same local baseline correction and scaled with the normalization factor used in Fig. S4(b). Compared with pure HPAM, the HPAM–SiO_2 mixture exhibits a stronger and broader $O-H/N-H$ band, consistent with an enhanced hydrogen-bonding network. Taken together, the Amide I red shift in (b) and the broadened $O-H/N-H$ band in (c) support the conclusion that introducing SiO_2 enhances hydrogen bonding in the system.

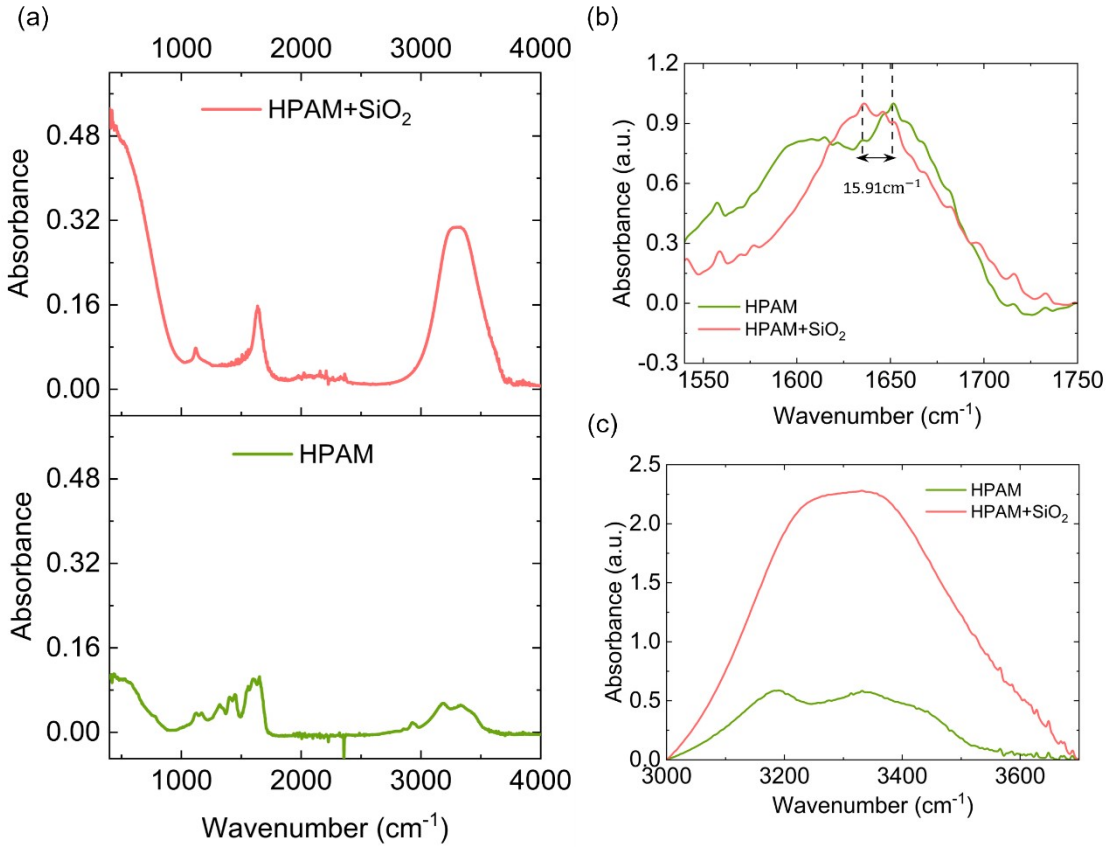

Fig. S4. FT-IR spectra of pure HPAM and the HPAM–SiO_2 mixture. (a) Raw spectra; (b) 1550–1750 cm^{-1} zoom-in after local linear baseline correction and Amide I peak-height normalization, showing an ~16 cm^{-1} red shift of Amide I; (c) 3000–3700 cm^{-1} zoom-in processed with the same local baseline correction and scaled using the normalization factor in (b), showing an enhanced $O-H/N-H$ band.

V. Supplementary rheology of 50 ppm HPAM–nanoparticle mixtures

To supplement the dilute-polymer regime, the complete apparent-viscosity–shear-rate curves are provided for 50 ppm polyacrylamide solutions containing nanoparticles at different concentrations (Fig. S5). The measurements were conducted using the same rheological protocol as described in the main text. The results indicate that, in dilute polymer solutions, an apparent viscosity increase is induced by nanoparticle addition, together with a thickening plateau at higher nanoparticle concentrations and an eventual reversal. These data allow readers to examine in detail the evolution of the viscosity increase.

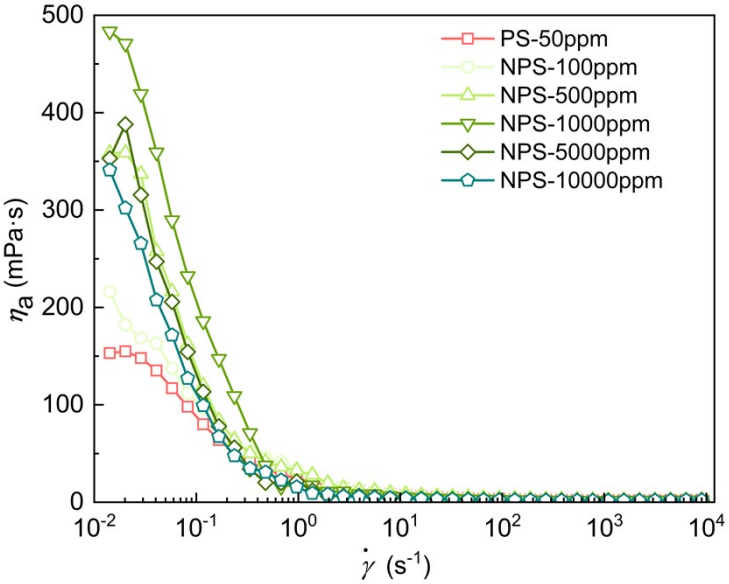

Fig. S5. Apparent viscosity as a function of shear rate for 50 ppm polyacrylamide solution (PS-50 ppm) with nanoparticles added at different concentrations (100–10,000 ppm).